JNeurosci Accepted Manuscript

This Accepted Manuscript has not been copyedited and formatted. The final version may differ from this version.

JNeurosci
THE JOURNAL OF NEUROSCIENCE

Research Articles: Neurobiology of Disease

Disease progression-dependent effects of TREM2 deficiency in a mouse model of Alzheimer's disease

Taylor R. Jay[1,2], Anna M. Hirsch[1], Margaret L. Broihier[1], Crystal M. Miller[2], Lee E. Neilson[1], Richard M. Ransohoff[3], Bruce T. Lamb[1,4] and Gary E. Landreth[1]

[1]*Department of Neurosciences, Case Western Reserve University, 44106*
[2]*Department of Neurosciences, The Cleveland Clinic Lerner Research Institute, Cleveland, OH, 44195*
[3]*Neuroimmunology/Discovery Biology, Biogen, 02142*
[4]*Stark Neurosciences Research Institute, Indiana University, 46202*

DOI: 10.1523/JNEUROSCI.2110-16.2016

Received: 30 June 2016

Revised: 30 November 2016

Accepted: 5 December 2016

Published: 9 December 2016

Author contributions: T.R.J., A.M.H., M.B., B.T.L., and G.E.L. designed research; T.R.J., A.M.H., M.B., and C.M. performed research; T.R.J., A.M.H., M.B., and L.E.N. analyzed data; T.R.J. wrote the paper; R.M.R. contributed unpublished reagents/analytic tools.

Conflict of Interest: None

This work was supported by the Alzheimer's Association (BFG-15-364590 to GEL), the Jane and Lee Seidman Fund, generous donations from Chet and Jane Scholtz and Dave and Susan Roberts (to BTL), NIA grant RF1 AG051495 (BTL and GEL), NIA grant R01 AG050597 (to GEL), NIA National Research Service Award F31 AG048704 (to TRJ), and Case Western Reserve University Neurosciences training grant T32 NS067431 (to TRJ). We thank the imaging core at Case Western Reserve University and the flow cytometry core at The Cleveland Clinic Lerner Research Institute for their technical support.

Corresponding author information: Dr. Gary E. Landreth, Department of Neurosciences, Case Western Reserve University, Cleveland, OH 44106, Phone Number: (216) 368-6101, Fax Number: (216) 368-4650, E-mail: gel2@case.edu

Cite as: J. Neurosci 2016; 10.1523/JNEUROSCI.2110-16.2016

Alerts: Sign up at www.jneurosci.org/cgi/alerts to receive customized email alerts when the fully formatted version of this article is published.

Accepted manuscripts are peer-reviewed but have not been through the copyediting, formatting, or proofreading process.

Copyright © 2016 the authors

JNeurosci Accepted Manuscript

1 **Disease progression-dependent effects of TREM2 deficiency in a mouse model**
2 **of Alzheimer's disease**

3 Taylor R. Jay[1,2], Anna M. Hirsch[1], Margaret L. Broihier[1], Crystal M. Miller[2], Lee E. Neilson[1],
4 Richard M. Ransohoff[3], Bruce T. Lamb[1,4], Gary E. Landreth[1]
5 [1]Department of Neurosciences, Case Western Reserve University, 44106
6 [2]Department of Neurosciences, The Cleveland Clinic Lerner Research Institute, Cleveland, OH, 44195
7 [3]Neuroimmunology/Discovery Biology, Biogen, 02142
8 [4]Stark Neurosciences Research Institute, Indiana University, 46202
9
10 Corresponding author information:
11 Dr. Gary E. Landreth
12 Department of Neurosciences
13 Case Western Reserve University
14 Cleveland, OH 44106
15 Phone Number: (216) 368-6101
16 Fax Number: (216) 368-4650
17 E-mail: gel2@case.edu
18
19 Abbreviated Title: Role of TREM2 throughout AD progression
20 Number of pages: 32
21 Number of figures: 6
22 Number of tables: 1
23 Number of words for Abstract: 167
24 Number of words for Introduction: 451
25 Number of words for Discussion: 1,374
26
27 Conflict of Interest: None
28
29 Acknowledgements: This work was supported by the Alzheimer's Association (BFG-15-364590 to GEL),
30 the Jane and Lee Seidman Fund, generous donations from Chet and Jane Scholtz and Dave and Susan
31 Roberts (to BTL), NIA grant RF1 AG051495 (BTL and GEL), NIA grant R01 AG050597 (to
32 GEL), NIA National Research Service Award F31 AG048704 (to TRJ), and Case Western Reserve
33 University Neurosciences training grant T32 NS067431 (to TRJ). We thank the imaging core at Case
34 Western Reserve University and the flow cytometry core at The Cleveland Clinic Lerner Research
35 Institute for their technical support.

JNeurosci Accepted Manuscript

36 **ABSTRACT:**

37 Neuroinflammation is an important contributor to Alzheimer's disease (AD) pathogenesis, as underscored
38 by the recent identification of immune-related genetic risk factors for AD, including coding variants in the
39 gene *triggering receptor expressed on myeloid cells 2 (TREM2)*. Understanding TREM2 function promises
40 to provide important insights into how neuroinflammation contributes to AD pathology. However, studies so
41 far have produced seemingly conflicting results, with reports that amyloid pathology can be both decreased
42 and increased in TREM2 deficient AD mouse models. In this study, we unify these previous findings by
43 demonstrating that TREM2 deficiency ameliorates amyloid pathology early, but exacerbates it late in disease
44 progression in the APPPS1-21 mouse model of AD. We also demonstrate that TREM2 deficiency decreases
45 plaque-associated myeloid cell accumulation by reducing cell proliferation, specifically late in pathology. In
46 addition, TREM2 deficiency reduces myeloid cell internalization of amyloid throughout pathology, but
47 selectively decreases inflammation-related gene transcript levels late in disease progression. Together, these
48 results suggest that TREM2 plays distinct functional roles at different stages in AD pathology.

JNeurosci Accepted Manuscript

49 **SIGNIFICANCE:**

50 Alzheimer's disease (AD) is a devastating neurodegenerative disorder, and there are currently no effective
51 treatments which modify disease progression. However, the recent identification of genetic risk factors for
52 AD promise to provide new insight into AD biology and possible new therapeutic targets. Among these risk
53 factors, variants in the gene *TREM2* confer greatly elevated risk for developing the disease. We demonstrate
54 that TREM2 deficiency has opposing effects on AD-related pathologies at early and late stages of disease
55 progression, unifying previous work in the field. In addition, we examine how TREM2 effects the function
56 of the brain immune cell populations in which it's expressed throughout disease progression to understand
57 possible mechanisms underlying its differential impacts on pathology.

58

JNeurosci Accepted Manuscript

59 **INTRODUCTION**

60 Alzheimer's disease (AD) is characterized by a robust neuroinflammatory response (McGeer
61 et al., 1987; Itagaki et al., 1989; Heneka et al., 2015). In the past several years, genetic studies have
62 identified variants in immune-related genes which confer risk for developing AD (Karch and
63 Goate, 2015), directly implicating this neuroinflammatory response in AD pathogenesis. Of these
64 risk factors, coding variants in the gene *triggering receptor expressed on myeloid cells 2* (*TREM2*)
65 confer the highest AD risk (Guerreiro et al., 2013; Jonsson et al., 2013; Lill et al., 2015). *TREM2*
66 encodes a receptor that's exclusively expressed on immune cells within the brain (Schmid et al.,
67 2002; Colonna, 2003), and, in AD, is upregulated by plaque-associated myeloid cells (Frank et al.,
68 2008; Melchior et al., 2010; Jay et al., 2015). These brain myeloid cells include microglia, brain
69 resident macrophages and, in the context of Alzheimer's disease, may also include macrophages
70 derived from peripheral monocytes (El Khoury et al., 2007; Gate et al., 2010; Koronyo et al.,
71 2015). *TREM2*'s genetic linkage to AD suggests that these myeloid cells play an important role in
72 AD pathogenesis. Understanding more about TREM2 expression and function within these cells
73 promises to provide insights into the complex roles that immune cells perform in the context of
74 AD.

75 In order to investigate the functional role of TREM2 and assess its impact on AD pathology,
76 recent studies examined TREM2 deficient AD mouse models. Collectively, these studies
77 demonstrated that TREM2 deficiency reduces accumulation of myeloid cells around plaques
78 (Ulrich et al., 2014; Jay et al., 2015; Wang et al., 2015) and attenuates inflammation-related gene
79 expression (Jay et al., 2015; Wang et al., 2015). However, these studies differed in their
80 conclusions regarding the impact of TREM2 deficiency on amyloid pathology (Tanzi, 2015). Jay
81 and colleagues (2015) reported reduced amyloid pathology early in disease progression in the
82 hippocampus of 4-month-old APPPS1;*Trem2*$^{-/-}$ mice, whereas Wang and colleagues (2015) found
83 no difference in amyloid pathology in the hippocampus of 4-month-old 5XFAD;*Trem2*$^{-/-}$ mice

JNeurosci Accepted Manuscript

84 compared to controls (Wang et al., 2016), but increased amyloid accumulation at 8 months of age
85 (Wang et al., 2016) (summarized in Table 1). These opposing findings raised concerns in the field
86 about possible model-specific or facility-dependent (Montalvo et al., 2013) effects of TREM2
87 deficiency on pathology. Because these studies examined the effects of TREM2 deficiency at
88 different time points in disease progression, these divergent findings could also be explained by
89 distinct roles of TREM2 at different stages of pathology.

90 In this study, we assess the functional role of TREM2 in the APPPS1 (Radde et al., 2006)
91 AD mouse model at early and late stages of disease to determine whether TREM2 might play a
92 disease progression-dependent role in modifying AD pathology and myeloid cell function.

93

94 **MATERIALS AND METHODS**

95 **Mice**

96 The APPPS1-21 (APPPS1) mouse model of Alzheimer's disease (provided by Mathias Jucker) expresses
97 human familial mutations in APP (K670M/N671L) and PSEN1 (L166P) under the control of the Thy1
98 promoter (Radde et al., 2006). These mice were crossed with *Trem2*$^{-/-}$ mice (TREM2tm1(KOMP)Vlcg) from
99 the NIH knock-out mouse project which express a lacZ reporter in place of exons 2, 3 and part of 4. These
100 mice were previously characterized to lack TREM2 expression (Jay et al., 2015). All mice were maintained
101 on a B6 background. Because previous studies have suggested that sex may impact the time course of
102 pathology development in this model, both sexes of mice were used for these experiments. The number of
103 each sex used in each experiment is indicated in the figure legend. Mice were housed in the AALAC
104 accredited facility in the Cleveland Clinic Biological Resources Unit and all experimental procedures were
105 approved by the Cleveland Clinic Foundation IACUC committee.

106 **Quantitative RT-PCR**

JNeurosci Accepted Manuscript

107 Mice were perfused with PBS, cortices dissected and snap frozen on dry ice. Cortices were homogenized in
108 PBS with 1% NP-40, 0.5% sodium deoxycholate and 0.1% SDS. Lysates were added to an equal volume of
109 RNA-Bee and kept at -80°C until use. RNA was isolated using chloroform extraction and purified using the
110 Purelink RNA Mini Kit (Life Technologies). Samples were treated with an on-column DNAse Purelink kit
111 (Life Technologies). cDNA was prepared from 500ng of RNA using a QuantiTech Reverse Transcription kit
112 (Qiagen) and qPCR performed using the StepOne Plus Real Time PCR system (Life Technologies) using
113 Taqman assays. Relative gene expression is graphed as fold change gene expression and ΔC_T values were
114 used for statistical analyses and are reported in the results for each genotype.

115 **Immunohistochemistry**

116 Mice were deeply anesthetized with ketamine xylazine and perfused with ice cold PBS. Brains were
117 removed and one hemisphere drop fixed in 4% PFA at 4°C overnight and cryoprotected in 30% sucrose
118 before snap freezing in OCT. Brains were crysosectioned into 30µm sections and stored at 4°C in PBS
119 until use. For immunofluoresecent staining, slices were permeabilized in PBS with 0.1% Triton-X and
120 then antigen retrieval was performed using 10mM sodium citrate with 0.5% Tween pH 6.0 at 85°C for
121 15min and then at room temperature for 30min. Slices were blocked in 5% NGS/0.3% TritonX-100 in 1x
122 PBS for 1 hour and then incubated in the following primary antibodies overnight at 4°C: 6E10 (Covance
123 1:1000), Iba1 (Wako 1:1000), GFAP (Sigma-Aldrich 1:1000), S100β (R&D Systems 1:500). Slices were
124 incubated with Alexa-fluor conjugated secondary antibodies at a 1:1000 concentration for 1 hour at room
125 temperature. Mouse on mouse blocking reagent (Vector Laboratories) was added to the blocking solution
126 for all antibodies raised in mouse or rat. Slices were mounted using Prolong Gold. Cleaved caspase 3
127 staining (Cell Signaling 1:100) was performed as described except antigen retrieval was performed using
128 Reveal Decloaker (Biocare Medical) at 85°C for 15min and then at room temperature for 30min and
129 sections were incubated in primary antibody for 48 hours. BrdU staining (Abcam 1:50) was performed as
130 described above except following antigen retrieval, sections were incubated in 2M HCl at 37°C for 20min
131 and then incubated in 0.1M sodium borate for 10min at room temperature prior to blocking.

JNeurosci Accepted Manuscript

132 Immunohistochemistry for CD45 (ABD Serotec 1:500) followed the same procedure with the exception of
133 incubation in 1% H_2O_2 in PBS for 30 minutes following antigen retrieval, and biotinylated secondary
134 antibodies were used at a 1:200 concentration. Vectastain Elite ABC kit (Vector) was added to sections for 1
135 hour followed by incubation with diaminobenzidine with nickel chloride. Sections were co-stained where
136 indicated with Congo Red which has previously been used to characterize amyloid pathology in this AD
137 model (Radde et al., 2006). A 1% w/v solution of Congo Red was prepared in 80% ethanol and allowed to
138 stir overnight prior to being filtered. Sections were incubated in this Congo Red solution for 1 hour, then
139 dehydrated in 70%, 95% and 100% ethanol and the tissue cleared in xylene. Slices were mounted using
140 Permount.

141 Brightfield images were acquired on a Leica DMLS microscope (Leica Biosystems) using a QImaging
142 camera and QCapture Software (QImaging). Whole brain images were acquired using a Lecia SCN400F
143 with a motorized stage with Leica SCN Software. Confocal images were acquired on a LSM 510 META
144 microscope. 10-30 sections 1µm apart were stacked and reconstructed using Image J.

145 **Image Analysis**

146 GFAP, S100β and CD45 expression was assessed by determining the immunoreactive area around
147 plaques. For these analyses, one lateral and one medial section were matched for each animal. Two
148 representative fields, one in the motor cortex and one in the frontal cortex, were acquired for each
149 slice. Individual regions of interest were defined by taking a circle 100µm in diameter centered in the
150 middle of each plaque in the field of view. These areas were then thresholded manually by a blinded
151 observer to distinguish immunoreactivity from background. The percent immunoreactive area within
152 each region of interest was recorded for each plaque and averaged within each field of view. These
153 values were then averaged across images to produce the percent immunoreactive area / plaque value
154 reported for each mouse.

155 The number of Iba1+ cells per plaque was quantified. For these analyses, 3 slices from medial to

JNeurosci Accepted Manuscript

156 lateral were matched and stained for each animal. Two images were acquired per slice in randomized
157 regions of the cortex by an experimenter blinded to genotype. Images were taken 1μm apart from the
158 first plane containing a plaque in the field of view through the last. Z stacks were projected from
159 these images and regions of interest defined around each plaque as described above. An independent
160 blinded observer quantified the number of Iba1+ cell bodies within that defined region of interest.
161 These numbers were averaged for each image, and then the images averaged together to define the
162 number of Iba1+ cells per plaque.

163 The number of CD45+ cells / mm^2 was quantified. For these analyses, slide scans of whole cortices
164 from one medial and one lateral matched sagittal slice were acquired. A blinded observer manually
165 counted the number of CD45+ cells across the cortex in each section and recorded the area of the
166 cortex within each section. The number of CD45+ cells / mm^2 was recorded for each section and
167 averaged across both sections for each animal.

168 The number of Thioflavin S+ plaques / mm^2 was quantified. For these analyses, every 12th section
169 across the hemibrain was stained with ThioS and images of the whole cortex in each section were
170 acquired on a slide scanner. A blinded observer recorded the area of each cortex and the number of
171 ThioS+ plaques per cortex for each section. The number of ThioS+ plaques / mm^2 was determined for
172 each section and these values were averaged across sections to determine the number of ThioS+
173 plaques / mm^2 for each animal.

174 6E10 immunoreactive area and plaque size were quantified from slide scanned images of the cortex
175 from every 12th section across the hemibrain. A blinded observer quantified these images by making
176 regions of interest around each plaque and determining the total 6E10 immunoreactive area for each
177 plaque within each cortical section. The 6E10+ area for each plaque was then added together to yield
178 the total 6E10+ area for each cortical section. This approach was used instead of making a global
179 threshold across the whole cortex to avoid thresholding edge effects from tiling and non-specific

JNeurosci Accepted Manuscript

180 binding to blood vessels. This total 6E10+ area was divided by the total area of the cortical section to
181 determine the percent 6E10+ area for each slice. This number was averaged across all sections for
182 each animal. Plaque size was determined from the same data, using the area recorded for each plaque
183 in the analysis above and averaging these across each section. The averages of these sections were
184 then recorded as average plaque area, given in arbitrary units.

185 The number of BrdU+ Iba1+ cells per cortical section was quantified. For these analyses, matched
186 lateral and medial sections were imaged on a slide scanner and images of Iba1 and BrdU were
187 overlaid. A blinded observer quantified the number of BrdU+ Iba1+ cells in each cortical section and
188 these values were averaged between sections. Ki67+ Iba1+ cells were quantified in the same manner.

189 **Flow Cytometry**

190 Mice were anesthetized with ketamine xylazine and perfused with ice cold Hank's balanced salt
191 solution. Brains were chopped and digested using the Miltenyi Neural Dissociation kit at 37°C. Cells were
192 washed, strained and resuspended in a 30% Percoll solution. 10% FBS was overlayed and the myelin at
193 the interface removed following centrifugation. Cells collected at the bottom of the gradient were
194 resuspended in FACS buffer (PBS, 1% BSA, 0.1% NaN_3, 5mM EDTA) and filtered. Cells were blocked
195 with a 1:200 concentration of CD16/CD32 antibody (BD Pharmingen) for 10min. Samples were pooled
196 for unstained and single stained controls. Cells were stained with a mastermix of CD45:AX700
197 (BioLegend, 1:500) and CD11b:BV605 (BioLegend, 1:500). Cells were then fixed and permeabilized
198 using the BD Cytofix/Cytoperm kit and then exposed to 1M HCl at RT for 10min, spun down and
199 resuspended in 0.1M sodium borate for 5min. Cells were then stained in permeabilization buffer with BrdU
200 (Abcam, 1:100) for 30min at room temperature. Cells were then washed and resuspended in
201 permeabilization buffer containing 1:1000 concentration of Alexa-488 secondary at room temperature for
202 15min. Cells were resuspended in PBS and stored at 4°C overnight. Events were acquired on a BD
203 Fortessa SORP (BD Biosciences) and analyzed using FlowJo. For analysis, events were gated on single

JNeurosci Accepted Manuscript

204 cells and CD11b positive events. Samples with more than 5,000 CD11b positive events were included
205 in the analysis.

206 **Western Blotting**

207 Tissue was extracted and processed as described above, then were sonicated and centrifuged.
208 Protein concentration was determined using a BCA kit (Thermo Scientific). Proteins were boiled for 5
209 minutes at 95°C in sample buffer containing DTT. 30μg of protein per sample was loaded into 4-12%
210 Bis-Tris gels (Life Technologies) and run at 100V. Protein was transferred onto IR-compatible PVDF
211 membranes on ice in a Tris glycine buffer containing methanol at 100V for 1hr. Membranes were
212 blocked in a 1:1 dilution of TBS Odyssey Blocking Buffer : TBS for 1 hour at room temperature and
213 incubated with the indicated primary antibodies in blocking buffer overnight at 4°C: 6E10 (BioLegend
214 1:5000) or actin (Santa Cruz 1:1000). Membranes were washed in TBS and incubated in a 1:10,000
215 dilution of the appropriate IR dye conjugated secondary antibody in blocking buffer for 1 hour at room
216 temperature. Membranes were imaged and analyzed using the Odyssey imaging system. Each sample was
217 normalized to actin and the graphs represent these values normalized to the mean of the APPPS1;*Trem2*$^{+/+}$
218 group at each time point.

219 **Statistics**

220 Statistical analyses were performed using GraphPad Prism. While graphed together, experiments at 2 and
221 8 month time points were performed independently and thus statistical comparisons were only made
222 between genotypes within a given age. Two-sided, unpaired t-tests were used to determine statistical
223 differences between groups at each time point. Column statistics were performed to identify outliers and
224 these samples were excluded. Each n is a single biological replicate. Graphs represent the mean and error
225 bars denote the SEM. Statistical values in the text are expressed as: (mean ± SEM values for
226 APPPS1;*Trem2*$^{+/+}$ vs mean ± SEM values for APPPS1;*Trem2*$^{-/-}$, t(degrees of freedom)=t value, p value).
227 Power analyses were not used to determine group sizes, but the number of replicates included here are

JNeurosci Accepted Manuscript

228 comparable to those used in previous studies (Jay et al., 2016; Ulrich et al., 2015; Wang et al., 2015).
229 Mice from three separate cohorts were included for each group.

230

231 **RESULTS**

232 **Loss of TREM2 alters the temporal progression of amyloid pathology**

233 In order to longitudinally evaluate the effect of TREM2 deficiency on amyloid pathology, we
234 expanded on our previous work examining 4-month-old TREM2 deficient APPPS1 mice by assessing
235 amyloid plaque area and number in the cortex of 2- and 8-month-old APPPS1;*Trem2*$^{+/+}$ and
236 APPPS1;*Trem2*$^{-/-}$ mice. At 2 months of age, an early stage of amyloid deposition in the cortex of the
237 APPPS1 model, analysis of 6E10 immunoreactive area revealed a significant reduction in total plaque
238 area in TREM2 deficient mice (Figure 1e, representative images Figure 1a; WT 0.38±0.02 vs KO
239 0.23±0.05, $t(8)=2.8$, $p=0.021$). At 4 months of age, a midpoint in amyloid deposition in the cortex in the
240 APPPS1 mouse model, we previously reported that there were no significant differences in 6E10 area in
241 the cortex (Jay et al., 2015). When total plaque area was examined in the cortex at 8 months of age, a
242 relatively late time point in disease progression, we found a significant increase in 6E10 immunoreactive
243 area in TREM2 deficient mice (Figure 1e, representative images Figure 1b; WT 1.39±0.18 vs KO
244 3.04±0.38, $t(11)=3.7$, $p=0.004$). Together, these findings demonstrate that TREM2 deficiency reduces
245 cortical plaque area early but increases it late in disease progression (summarized in Table 1).

246 We next examined the effects of TREM2 deficiency on plaque number by quantifying the density
247 of Thioflavin S+ plaques in the cortex of 2- and 8-month old APPPS1;*Trem2*$^{+/+}$ and APPPS1;*Trem2*$^{-/-}$
248 mice. At 2 months of age, there was a trend toward a reduction in the density of Thioflavin S+ plaques in
249 TREM2 deficient mice compared to controls (Figure 1f, representative images Figure 1c; WT
250 0.095±0.006 vs KO 0.063±0.014, $t(12)=2.0$, $p=0.072$), in line with the significant reduction in plaque area
251 at that time point. At 8 months of age, we did not detect any significant differences in Thioflavin S+

JNeurosci Accepted Manuscript

252 plaque density in TREM2 deficient APPPS1 mice (Figure 1f, representative images Figure 1d; WT
253 0.13±0.01 vs KO 0.13±0.02, t(12)=0.1, p=0.930). These data suggest that TREM2 deficiency selectively
254 decreases plaque number at early stages of disease progression.

255 In order to address possible explanations for the increase in total plaque area without concomitant
256 changes in plaque number in TREM2 deficient mice at 8 months of age, we assessed whether the average
257 size of plaques in TREM2 deficient mice might be altered late stage in disease progression. Quantification
258 of average plaque size revealed no significant differences between 2-month-old APPPS1;*Trem2*$^{-/-}$ mice
259 compared to APPPS1;*Trem2*$^{+/+}$ mice (WT 7.07±0.98 vs KO 5.76±0.49, t(9)=1.3, p=0.240), but at 8
260 months of age, there was a striking increase in the average plaque size in TREM2 deficient mice (Figure
261 1g; WT 26.79±4.57 vs KO 60.99±9.79, t(9)=2.5, p=0.034). This is in line with recent findings
262 demonstrating that TREM2 deficiency can lead to increased diffuseness of plaques with greater fibril
263 extension (Wang et al., 2016; Yuan et al., 2016).

264 We wanted to determine whether these disease progression-dependent changes in amyloid
265 pathology observed in the cortex also occurred in other brain regions. We previously reported a significant
266 reduction in amyloid pathology in the hippocampus of 4-month-old TREM2 deficient APPPS1 mice
267 compared to controls (Jay et al., 2015), an early stage in pathology in that brain region. This led us to
268 examine whether amyloid plaque accumulation would be differentially affected at 8 months of age, a
269 midpoint in disease progression in the hippocampus. We found no significant differences in 6E10
270 immunoreactive area in the hippocampus of 8-month-old APPPS1;*Trem2*$^{-/-}$ mice compared to controls
271 (0.96±0.17 vs 1.52±0.29, t(11)=1.6, p=0.132). There was also a trend toward an increase in average
272 plaque size in the hippocampus of TREM2 deficient mice compared to controls (29.42±5.25 vs
273 62.71±11.43, t(9)=2.1, p=0.066) (summarized in Table 1). These results indicate that there is also a
274 disease-progression dependent effect of amyloid pathology in the hippocampus of APPPS1 mice, with
275 reductions in amyloid pathology early, but no significant changes at a midpoint in disease progression.

JNeurosci Accepted Manuscript

276 In order to ensure that these differences in amyloid pathology were not due to differences in
277 transgene expression, we assessed transcript (Figure 1h) and protein levels (Figure 1i-j) of human APP.
278 While there was a significant reduction in APP transcript levels in lysates from Trem2 deficient mice at 8
279 (WT 2.43±0.19 vs KO 1.45±0.25, t(9)=3.1, p=0.012) but not 2 months of age (WT 1.86±0.20 vs KO
280 1.89±0.15, t(10)=1.1, p=0.913), there were no significant alterations in APP protein levels at 2 (WT
281 1.00±0.06 vs KO 0.89±0.11, t(8)=0.9, p=0.374) or 8 months of age (WT 1.00±0.16 vs KO 1.31±0.20,
282 t(8)=1.2, p=0.258), suggesting that changes in transgene expression are not driving the changes in
283 pathology observed in this study.

284 Together, these data suggest a disease progression-dependent role for TREM2 on amyloid
285 pathology. TREM2 deficiency initially results in reduced amyloid pathology, but leads to increased plaque
286 area late in disease progression. These results are consistent with our previous findings as well as those
287 reported in TREM2-deficient mice using other AD mouse models (summarized in Table 1).

288 **TREM2 deficiency decreases the number of CD45^{hi} and plaque-associated myeloid cells**

289 Because TREM2 deficiency had opposing effects on amyloid plaque accumulation early and late in
290 disease progression, we assessed whether TREM2 deficiency might differentially affect myeloid cell
291 distribution and phenotype at these two time points. First, we examined gene expression of myeloid cell
292 markers in the cortex of 2- and 8-month old APPPS1;*Trem2*$^{+/+}$ and APPPS1;*Trem2*$^{-/-}$ mice to assess how
293 TREM2 deficiency impacted different myeloid cell subsets. There were no significant changes in
294 expression of these myeloid cell markers in 2-month-old TREM2 deficient mice compared to controls
295 (Figure 2a; PU.1 WT 11.63±0.17 vs KO 12.12±0.42, t(10)=1.1, p=0.304; Tmem119 WT 9.80±0.17 vs KO
296 9.93±0.19, t(10)=0.5, p=0.626; CD45 WT 14.60±0.32 vs KO 14.76±0.32, t(10)=0.3, p=0.735). However,
297 at 8 months of age, there were trends toward reductions in the expression of the myeloid cell transcription
298 factor PU.1 (WT 10.42±0.28 vs KO 11.14±0.20, t(9)=2.1, p=0.060) (Scott et al., 1994) and the previously
299 characterized microglia specific marker, Tmem119 (WT 8.64±0.09 vs KO 8.93±0.09, t(9)=2.1, p=0.060)

JNeurosci Accepted Manuscript

300 (Butovsky et al., 2014; Bennett et al., 2016), in TREM2 deficient mice (Figure 2a). Additionally, the
301 myeloid cell marker CD45 was significantly and substantially reduced in TREM2 deficient mice at 8
302 months of age (Figure 2a; WT 11.70±0.09 vs 13.60±0.24, $t(9)=5.7$, $p=0.0003$). Previous work showed that
303 TREM2 in APPPS1 mice and other AD models was expressed exclusively on myeloid cells expressing
304 high levels of CD45 throughout disease progression (Jay et al., 2015). Because of these previous findings
305 and the gene expression data in this study, we chose to distinguish myeloid cells subsets expressing high
306 ($CD45^{hi}$) and low ($CD45^{lo}$) levels of this marker in subsequent studies examining TREM2 function.

307 It was unclear whether the changes in gene expression of myeloid cell markers reflected a change
308 in the total number of cells within these myeloid cell populations or altered gene expression. To
309 distinguish these two possibilities, the numbers of myeloid cells in the cortex of 2- and 8-month-old
310 APPPS1;*Trem2*$^{+/+}$ and APPPS1;*Trem2*$^{-/-}$ were quantified. There were no significant differences in the
311 number of cells labeled with the pan-myeloid cell marker Iba1 in TREM2 deficient mice compared to
312 controls (data not shown). However, quantification of the number of $CD45^{hi}$ cells revealed a significant
313 reduction in this population in 2-month-old (WT 0.14±0.01 vs KO 0.02±0.005, $t(9)=16.2$, $p<0.0001$) and
314 8-month-old APPPS1;*Trem2*$^{-/-}$ mice compared to APPPS1;*Trem2*$^{+/+}$ controls (Figure 2b-d; WT 1.26±0.11
315 vs 0.15±0.03, $t(10)=10.2$, $p<0.0001$). Together, these data demonstrate that TREM2 deficiency affects
316 brain myeloid cell number, especially at late stages in disease progression and specifically within the
317 $CD45^{hi}$ myeloid cell subset in which TREM2 is known to be predominantly expressed.

318 It has been previously reported that TREM2 deficiency also affects accumulation of myeloid cells
319 around plaques (Ulrich et al., 2014; Jay et al., 2015b; Wang et al., 2015). We assessed whether TREM2
320 deficiency affected the accumulation of myeloid cells differentially at early and late stages in disease
321 progression. Analysis of $Iba1^{+}$ myeloid cell accumulation around $6E10^{+}$ plaques in 2-month-old (Figure
322 3a,c; WT 3.76±0.31 vs KO 1.75±0.21, $t(9)=5.5$, $p=0.0004$) and 8-month-old (Figure 3b,d; WT 9.39±0.55
323 vs KO 4.39±0.44, $t(4)=7.1$, $p=0.002$) TREM2 deficient mice revealed significant reductions in plaque-
324 associated myeloid cells at both time points (Figure 3e). Consistent with our findings that $CD45^{hi}$ cell

JNeurosci Accepted Manuscript

325 number was decreased in TREM2 deficient mice, analysis of CD45 immunoreactivity around Congo
326 Red+ plaques in 2-month-old (Figure 3f; WT 15.40±0.74 vs KO 3.85±0.61, $t(9)=12.2$, $p<0.0001$) and 8-
327 month-old (Figure 3g; WT 28.39±3.50 vs KO 6.05±1.18, $t(10)=6.0$, $p=0.0001$) mice also revealed a
328 significant reduction in accumulation of this myeloid cell subset around plaques in TREM2 deficient mice
329 at both time points (Figure 3h). Together, these results demonstrate reduced accumulation of $CD45^{hi}$
330 myeloid cells associated with plaques in TREM2 deficient mice at both early and late stages in disease
331 progression.

332 **TREM2 deficiency reduces myeloid cell proliferation at late stages in disease progression**

333 Due to the observed reduction in plaque-associated myeloid cells in TREM2 deficient mice
334 throughout the time course of pathology, we wanted to assess whether TREM2 deficiency drove this
335 reduction in plaque-associated cells through different mechanisms at early and late stages in disease
336 progression. In other disease contexts, TREM2 has been shown to play an important role in myeloid cell
337 proliferation (Otero et al., 2012; Cantoni et al., 2015; Poliani et al., 2015) which could contribute to a loss
338 of plaque-associated myeloid cells.

339 We assessed whether TREM2 deficiency contributes to myeloid cell loss in AD mice by impairing
340 myeloid cell proliferation. To examine proliferation, BrdU injections were administered every 24 hours
341 for 72 hours prior to sacrifice and the number of $BrdU^{+}$ $Iba1^{+}$ myeloid cells were quantified in the cortex
342 of APPPS1;*Trem2*$^{-/-}$ and APPPS1;*Trem2*$^{+/+}$ mice at 2 months (Figure 4a) and 8 months (Figure 4b) of age.
343 The numbers of proliferating cells were not significantly altered at 2 months of age (WT 16.50±2.5 vs KO
344 12.00±3.00, $t(3)=1.2$, $p=0.368$) but were significantly reduced in 8-month-old TREM2 deficient mice
345 compared to controls (Figure 4c; WT 74.80±3.08 vs KO 33.06±5.94, $t(12)=5.0$, $p=0.003$). An independent
346 evaluation of proliferation was performed by examining $Ki67^{+}$ $Iba1^{+}$ cell numbers. Similar to our BrdU
347 analysis, we found no change in proliferating cells per cortex in 2-month-old APPPS1;*Trem2*$^{+/+}$ and
348 APPPS1;*Trem2*$^{-/-}$ mice (WT 44.20±9.69 vs KO 37.83±8.59, $t(6)=0.4$, $p=0.673$), but a significant reduction

JNeurosci Accepted Manuscript

349 in TREM2 deficient mice compared to controls at 8 months of age (WT 17.38±3.08 vs KO 6.10±0.93,
350 $t(7)=3.9$, $p=0.006$).

351 Because TREM2 deficiency specifically decreased the number of $CD45^{hi}$ myeloid cells in APPPS1
352 mice, we wanted to examine whether proliferation was preferentially affected in this myeloid cell subset.
353 To assess this possibility, 6-9-month-old APPPS1;*Trem2*$^{+/+}$ mice were administered BrdU as described
354 above and brain myeloid cells were isolated and analyzed using flow cytometry. The cells were gated on
355 CD11b (Figure 4d) to select the total myeloid cell population and then divided into $CD45^{lo}$ and $CD45^{hi}$
356 populations (Figure 4e). Quantification of the percent of $BrdU^{+}$ cells within the $CD45^{hi}$ cell population
357 revealed few proliferating cells (0.43%) (Figure 4f). Rather, $BrdU^{+}$ cells were primarily identified within
358 the $CD45^{lo}$ microglial population (7.94%) (Figure 4g). These findings are consistent with the
359 interpretation that TREM2 deficiency affects $CD45^{hi}$ myeloid cell numbers throughout disease
360 progression, but has a specific impact on $CD45^{lo}$ myeloid cells late in disease pathology. This reduction in
361 $CD45^{lo}$ myeloid cell proliferation is likely a contributing factor to the loss of plaque-associated myeloid
362 cells selectively at this late time point, and suggests that TREM2 alters myeloid cell number early and late
363 in disease progression through different mechanisms. It remains to be determined whether this is due to
364 targeting of distinct myeloid cell subsets at different stages in pathology or whether TREM2 or myeloid
365 cell function in general might change throughout disease progression.

366 **TREM2 deficiency reduces amyloid internalization, astrocytosis and inflammatory gene expression**

367 Our findings indicate that TREM2 is important for proliferation of myeloid cells late in disease
368 progression, leading to a loss of plaque-associated myeloid cells in TREM2 deficient mice. We next
369 assessed whether TREM2 deficiency and loss of these cells would affect myeloid cell functions known to
370 be important modifiers of AD-related pathologies, including myeloid cell internalization of amyloid,
371 astrocytosis and inflammation. Because TREM2 has been shown to play an important role in phagocytosis
372 in other contexts (Takahashi et al., 2005; Hsieh et al., 2009; Kawabori et al., 2015), we assessed whether

JNeurosci Accepted Manuscript

373 TREM2 deficiency impacted myeloid cell internalization of amyloid plaques. Plaques and plaque-
374 associated myeloid cells were reconstructed from confocal stacks and the volume of 6E10 and Iba1
375 colocalization was quantified as a measure of 6E10 internalization within myeloid cells. This area was
376 normalized to the total plaque volume. At both 2 (Figure 5a; WT 14.09±2.31 vs KO 4.03±1.00, $t(4)=4.0$,
377 $p=0.016$) and 8 (Figure 5b; WT 12.36±2.64 vs KO 2.75±0.41, $t(4)=3.6$, $p=0.022$) months of age, TREM2
378 deficiency resulted in significantly reduced internalization of 6E10 within myeloid cells (Figure 5c).

379 Because amyloid internalization was impacted both early and late in pathology, changes in this
380 myeloid cell function could not explain the differential effects of TREM2 deficiency with regard to
381 amyloid accumulation early and late in disease progression. As such, we examined whether TREM2
382 deficiency might indirectly affect astrocyte activation and accumulation around plaques differentially at
383 these two time points. The total immunoreactive area of the astrocyte marker GFAP around $6E10^+$ plaques
384 at 2 (Figure 6a; WT 5.43±1.15 vs KO 0.72±0.24, $t(9)=4.4$, $p=0.002$) and 8 (Figure 6b; WT 26.74±2.30 vs
385 KO 18.60±2.30, $t(10)=2.6$, $p=0.027$) months of age was significantly reduced (Figure 6c) in TREM2
386 deficient mice. S100β expression has been used in other disease contexts to distinguish whether changes
387 in GFAP expression reflect altered astrocyte activation or are due to a change in the distribution of
388 astrocytes (Kang et al., 2014). In order to assess whether the changes in GFAP expression observed here
389 were due to a reduction in plaque-proximal astrocytes, expression of the pan-astrocyte marker S100β was
390 also examined in 2-month-old (Figure 6d; WT 5.83±0.30 vs KO 6.43±0.29, $t(9)=1.4$, $p=0.185$) and 8-
391 month-old (Figure 6e; WT 10.47±0.76 vs KO 11.22±0.71, $t(9)=0.7$, $p=0.498$) TREM2 deficient mice.
392 There were no significant changes in S100β immunoreactive area at either time point (Figure 6f),
393 suggesting that TREM2 deficiency likely affects the activation of astrocytes rather than astrocyte
394 distribution in the brains of AD mice.

395 Finally, we assessed whether these changes in myeloid cell accumulation and astrocytosis resulted
396 in reduced expression of inflammation-related genes. There were no significant changes in expression
397 levels of several pro- or anti-inflammatory genes in 2-month-old APPPS1;*Trem2*$^{-/-}$ mice compared to

JNeurosci Accepted Manuscript

398 APPPS1;*Trem2*$^{+/+}$ controls (Figure 6g; IL1β WT 14.31±0.47 vs KO 15.11±0.39, t(10)=1.3, p=0.215; IL6
399 WT 15.52±0.37 vs KO 15.35±0.50, t(10)=0.3, p=0.781; iNOS WT 14.19±0.23 vs KO 14.29±0.16,
400 t(10)=0.3, p=0.751; Ym1 WT 15.20±0.70 vs KO 15.37±0.41, t(10)=0.2, p=0.841; Fizz1 WT 14.80±0.29
401 vs KO 14.95±0.68, t(10)=0.2, p=0.847; Arg1 WT 15.26±0.66 vs KO 15.05±0.23, t(10)=0.3, p=0.767).
402 However, there was a significant reduction in inflammatory genes IL1β (WT 14.43±0.29 vs KO
403 16.17±0.19, t(9)=5.2, p=0.0005) and TNFα (WT 13.07±0.30 vs KO 15.14±0.40, t(9)=3.6, p=0.006) and a
404 significant increase in the IL4/IL13 response marker Fizz1 (WT 16.41±0.14 vs KO 14.99±0.35, t(9)=2.9,
405 p=0.016) in TREM2 deficient mice at 8 months of age, but no significant changes in other genes
406 examined (IL6 WT 16.18±0.24 vs KO 16.39±0.20, t(9)=0.7, p=0.527; iNOS WT 14.87±0.09 vs KO
407 15.31±0.22, t(9)=0.6, p=0.180; Ym1 WT 14.42±0.45 vs KO 14.82±0.40, t(9)=0.6, p=0.545; Arg1 WT
408 15.62±0.57 vs KO 15.55±0.16, t(8)=0.1, p=0.894). While myeloid cell accumulation and astrocytosis
409 were reduced at both the 2 and 8 month time points, we observed an overall reduction in inflammation
410 related transcript levels selectively in 8-month-old TREM2 deficient mice. This selective decrease in
411 inflammation could contribute to the differential impact of TREM2 deficiency on pathology at early and
412 late stages in disease progression, but additional studies will be required to determine the full array of
413 changes in myeloid cell functions that contribute to these effects.

414

415 **DISCUSSION**

416 We report that TREM2 deficiency has a disease-progression-dependent effect on amyloid
417 pathology and on AD-related myeloid cell functions. We found that loss of TREM2 results in a reduction
418 in plaque number and area early in disease progression, but increased plaque size and area late in
419 pathology. TREM2 deficiency decreased accumulation of myeloid cells around plaques and total numbers
420 of CD45^{hi} myeloid cells. Reduced cell proliferation contributed to these changes specifically at late stages
421 of pathology. TREM2 deficiency also reduced myeloid cell internalization of amyloid resulting in a

JNeurosci Accepted Manuscript

422 secondary effect of reduced astrocytosis at all time points examined. We found that mice lacking TREM2
423 exhibited selectively reduced inflammatory gene expression at late stages of pathology.

424 Our findings demonstrate that TREM2 deficiency has opposing effects on plaque burden as a
425 function of disease progression. This unifies the seemingly contradictory findings in the current literature.
426 Our previous work evaluated changes in amyloid pathology in 4-month-old APPPS1 TREM2 deficient
427 mice and reported no changes in the cortex, but significant reductions in the hippocampus, which is at an
428 early stage of pathology development at that time point (Jay et al., 2015). However, others have reported
429 no changes in amyloid pathology in the hippocampus of TREM2 deficient 5XFAD mice at 4 months of
430 age, a midpoint in disease progression in the 5XFAD model (Wang et al., 2016), and a significant increase
431 in pathology in the hippocampus of TREM2 deficient 8-month-old 5XFAD mice (Wang et al., 2015).
432 These opposing effects of TREM2 deficiency on amyloid pathology raised concerns about possible
433 differences between AD models or TREM2 knockout lines. However, our results here support that these
434 opposing results may instead reflect a disease progression dependent impact of TREM2 deficiency on
435 amyloid pathology. The possibility that TREM2 plays a time-dependent role in disease progression has
436 also been supported by other work examining the effects of TREM2 overexpression in AD mice. Jiang
437 and colleagues reported alterations in amyloid pathology in AD mice in which TREM2 was overexpressed
438 at early stages in disease progression (Jiang et al., 2014), but more recently showed that overexpression of
439 TREM2 at later stages in pathology did not significantly alter amyloid accumulation (Jiang et al., 2016).
440 The disease stage-dependent role of TREM2 on AD pathology presented here reconciles these previous
441 findings, and together with other work in the field, suggests that TREM2 deficiency reduces amyloid
442 pathology early but increases it late in disease progression.

443 While our findings are in line with the known data from human TREM2 variant carriers as well as
444 those using other strategies to alter TREM2 expression in AD mouse models, we have not definitively
445 demonstrated whether this TREM2 deletion model impacts expression of other gene transcripts in this
446 locus. The TREM2 locus also contains several immune-related genes, including some implicated in

JNeurosci Accepted Manuscript

447 altering AD risk and pathology such as TREM1 (Replogle et al., 2015) and TREML2 (Benitez et al.,
448 2014) and it is possible that expression of these or other transcripts could be impacted by deletion of
449 unrecognized regulatory sequences in our model for TREM2 deficiency. To exclude this possibility, and
450 to more closely model changes in TREM2 function which occur in human AD, it will be important to
451 make mouse models expressing human TREM2 variants, including those known to promote loss of
452 protein function like Q33X to validate findings from the TREM2 KO models reported so far, and those
453 that may not confer a full loss of function phenotype such as R47H (Kleinberger et al., 2014). These
454 models could provide insight into whether TREM2 deficiency fully models the effect of human AD risk
455 variants.

456 In this study, we demonstrate that TREM2 deficiency affects some aspects of myeloid cell function
457 in a consistent manner throughout disease progression, including myeloid cell accumulation around
458 plaques, phagocytosis and induction of astrocytosis. For that reason, differential effects of TREM2-
459 deficiency on myeloid cell functions cannot explain differential effects on amyloid pathology at early and
460 late time points. However, it remains possible that these alterations in myeloid cell distribution and
461 phenotype could have opposing impacts on amyloid accumulation at different stages of pathology.
462 Heneka and colleagues (2015) suggested that myeloid cell activation could play divergent roles early and
463 late in disease progression, which they proposed could underlie different results from clinical trials
464 examining use of immune-targeted therapeutics such as NSAIDs and Aβ immunotherapy at different
465 stages in disease progression. If this is the case, then understanding how immune-related functions
466 differentially regulate pathology at early and late stages of AD will be crucial to decipher the biology of
467 inflammation in the process of neurodegeneration, and to design effective inflammation-targeted
468 therapeutics. Studying how similar effects of TREM2 deficiency early and late in disease progression
469 result in opposing pathological outcomes could provide a platform to study how common myeloid cell
470 functions might play different roles throughout AD progression.

471 In addition to these consistent effects on myeloid cell function throughout progression, TREM2

JNeurosci Accepted Manuscript

472 deficiency does exhibit stage-specific effects on myeloid cell function. Specifically, alterations in
473 inflammatory gene expression were selectively altered late in pathology. Several recent studies have
474 demonstrated that reduced inflammation can exacerbate amyloid pathology (Guillot-Sestier et al.;
475 Chakrabarty et al., 2015). Thus, it is possible that reduced inflammation in TREM2 deficient mice late in
476 disease progression leads to the increases in amyloid accumulation observed at that time point. In this
477 study, we examined a small subset of the possible inflammation-related pathways altered by TREM2
478 deficiency. Future studies will be required to examine more broadly which pathways are altered in
479 TREM2 deficient mice and to define how changes in these pathways contribute to amyloid pathology.

480 TREM2 deficiency also reduced proliferation selectively at late stages in AD pathology.
481 Interestingly, we found that proliferation occurred specifically within $CD45^{lo}$ myeloid cells. However, we
482 previously reported that TREM2 is predominantly expressed on $CD45^{hi}$ macrophages in the AD brain
483 throughout the progression of pathology (Jay et al., 2015a). Our previous work based on marker
484 expression and our unpublished findings using bone marrow chimeras are consistent with the
485 identification of these cells as macrophages derived from peripheral monocytes. Therefore, one possible
486 explanation for the stage-dependent role of TREM2 deficiency on amyloid pathology is that TREM2
487 deficiency affects different myeloid cell subsets at different stages of pathology. TREM2 deficiency first
488 affects $CD45^{hi}$ myeloid cells where it is primarily expressed, but later loss of these $CD45^{hi}$ cells also
489 impacts the function of the $CD45^{lo}$ myeloid cells, reducing their proliferation and potentially altering other
490 AD-related phenotypes. If these subsets are indeed reflective of different cell origins, these data suggest
491 that opposing impacts of TREM2 on resident microglia and peripherally derived macrophages could
492 underlie its changing role throughout disease progression. Moving forward, it will be important to use
493 conditional TREM2 knockout models to definitively examine the effects of TREM2 deficiency in specific
494 myeloid cell populations throughout disease progression.

495 Taken together, we propose that TREM2 deficiency first results in loss of $CD45^{hi}$ myeloid cells
496 from the AD brain. These cells may normally play an important role in altering the local brain

JNeurosci Accepted Manuscript

497 microenvironment in AD, inducing a local inflammatory response in cells surrounding amyloid plaques.
498 Loss of these $CD45^{hi}$ myeloid cells results in reduced activation of plaque-associated astrocytes and, later
499 in disease progression, decreased activation and proliferation of $CD45^{lo}$ microglia. The reduction in
500 $CD45^{hi}$ myeloid cells mediated by TREM2 deficiency initially results in decreased amyloid pathology
501 through mechanisms which are not yet understood. However, later in disease progression, when $CD45^{lo}$
502 myeloid cell function is also impacted, reduced amyloid internalization and decreased inflammatory gene
503 transcription likely contribute to increased plaque size, and an overall increase in amyloid accumulation.

504 Since the identification of TREM2 variants as risk factors for AD, there has been substantial
505 interest in TREM2 as a potential inflammation-related therapeutic target. Recognizing the dual role for
506 TREM2 function early and late in disease progression provides important insights into the underlying
507 biology of TREM2 in AD and suggests new considerations in the development of TREM2-directed
508 therapeutics. This study suggests that trials using TREM2-directed therapies will have to carefully
509 consider the disease stage being targeted. The time point in progression at which these therapeutics are
510 delivered could critically affect clinical outcomes. These findings also suggest that disease progression
511 might be an important factor to consider in the use of inflammation- or immune cell-targeted therapeutics
512 in general in the context of AD.

JNeurosci Accepted Manuscript

513 **REFERENCES**
514

515 Benitez BA et al. (2014) Missense variant in TREML2 protects against Alzheimer's disease. Neurobiology
516 of Aging 35(6): 1510e19-26.

517 Bennett ML, Bennett FC, Liddelow SA, Ajami B, Zamanian JL, Fernhoff NB, Mulinyawe SB, Bohlen CJ,
518 Adil A, Tucker A, Weissman IL, Chang EF, Li G, Grant GA, Gephart MGH, Barres BA (2016)
519 New tools for studying microglia in the mouse and human CNS. Proceedings of the National
520 Academy of Sciences of the United States of America 113:E1738-E1746.

521 Butovsky O, Jedrychowski MP, Moore CS, Cialic R, Lanser AJ, Gabriely G, Koeglsperger T, Dake B, Wu
522 PM, Doykan CE, Fanek Z, Liu L, Chen Z, Rothstein JD, Ransohoff RM, Gygi SP, Antel JP,
523 Weiner HL (2014) Identification of a Unique TGF-β Dependent Molecular and Functional
524 Signature in Microglia. Nature neuroscience 17:131-143.

525 Cantoni C, Bollman B, Licastro D, Xie M, Mikesell R, Schmidt R, Yuede CM, Galimberti D, Olivecrona
526 G, Klein RS, Cross AH, Otero K, Piccio L (2015) TREM2 regulates microglial cell activation in
527 response to demyelination in vivo. Acta Neuropathol 129:429-447.

528 Chakrabarty P, Li A, Ceballos-Diaz C, Eddy JA, Funk CC, Moore B, DiNunno N, Rosario AM, Cruz PE,
529 Verbeeck C, Sacino A, Nix S, Janus C, Price ND, Das P, Golde TE (2015) IL-10 alters
530 immunoproteostasis in APP mice, increasing plaque burden and worsening cognitive behavior.
531 Neuron 85:519-533.

532 Chiu Isaac M, Morimoto Emiko TA, Goodarzi H, Liao Jennifer T, O'Keeffe S, Phatnani Hemali P, Muratet
533 M, Carroll Michael C, Levy S, Tavazoie S, Myers Richard M, Maniatis T A (2013)
534 Neurodegeneration-Specific Gene-Expression Signature of Acutely Isolated Microglia from an
535 Amyotrophic Lateral Sclerosis Mouse Model. Cell Reports 4:385-401.

536 Colonna M (2003) TREMs in the immune system and beyond. Nat Rev Immunol 3:445-453.

537 El Khoury J, Toft M, Hickman SE, Means TK, Terada K, Geula C, Luster AD (2007) Ccr2 deficiency
538 impairs microglial accumulation and accelerates progression of Alzheimer-like disease. Nat Med
539 13:432-438.

JNeurosci Accepted Manuscript

540 Frank S, Burbach GJ, Bonin M, Walter M, Streit W, Bechmann I, Deller T (2008) TREM2 is upregulated
541 in amyloid plaque-associated microglia in aged APP23 transgenic mice. Glia 56:1438-1447.
542 Gate D, Rezai-Zadeh K, Jodry D, Rentsendorj A, Town T (2010) Macrophages in Alzheimer's disease: the
543 blood-borne identity. Journal of Neural Transmission 117:961-970.
544 Gibot S, Kolopp-Sarda M-N, Béné M-C, Bollaert P-E, Lozniewski A, Mory F, Levy B, Faure GC (2004) A
545 Soluble Form of the Triggering Receptor Expressed on Myeloid Cells-1 Modulates the
546 Inflammatory Response in Murine Sepsis. The Journal of Experimental Medicine 200:1419-1426.
547 Guerreiro R et al. (2013) TREM2 variants in Alzheimer's disease. N Engl J Med 368:117-127.
548 Guillot-Sestier M-V, Doty Kevin R, Gate D, Rodriguez J, Jr., Leung Brian P, Rezai-Zadeh K, Town T
549 (2015) Deficiency Rebalances Innate Immunity to Mitigate Alzheimer-Like Pathology. Neuron
550 85:534-548.
551 Heneka MT, Carson MJ, Khoury J, Landreth GE, Brosseron F, Feinstein DL (2015) Neuroinflammation in
552 Alzheimer's disease. Lancet Neurol 14.
553 Heslegrave A, Heywood W, Paterson R, Magdalinou N, Svensson J, Johansson P, Ohrfelt A, Blennow K,
554 Hardy J, Schott J, Mills K, Zetterberg H (2016) Increased cerebrospinal fluid soluble TREM2
555 concentration in Alzheimer's disease. Mol Neurodegener 11:3.
556 Hickman SE, Kingery ND, Ohsumi TK, Borowsky ML, Wang LC, Means TK, El Khoury J (2013) The
557 microglial sensome revealed by direct RNA sequencing. Nat Neurosci 16:1896-1905.
558 Hsieh CL, Koike M, Spusta SC, Niemi EC, Yenari M, Nakamura MC, Seaman WE (2009) A role for
559 TREM2 ligands in the phagocytosis of apoptotic neuronal cells by microglia. J Neurochem
560 109:1144-1156.
561 Itagaki S, McGeer PL, Akiyama H, Zhu S, Selkoe D (1989) Relationship of microglia and astrocytes to
562 amyloid deposits of Alzheimer disease. Journal of Neuroimmunology 24:173-182.
563 Jay TR, Miller CM, Cheng PJ, Graham LC, Bemiller S, Broihier ML, Xu G, Margevicius D, Karlo JC,
564 Sousa GL, Cotleur AC, Butovsky O, Bekris L, Staugaitis SM, Leverenz JB, Pimplikar SW,
565 Landreth GE, Howell GR, Ransohoff RM, Lamb BT (2015) TREM2 deficiency eliminates

JNeurosci Accepted Manuscript

566 TREM2+ inflammatory macrophages and ameliorates pathology in Alzheimer's disease mouse
567 models. J Exp Med 212:287-295.
568 Jiang T, Wan Y, Zhang YD, Zhou JS, Gao Q, Zhu XC, Shi JQ, Lu H, Tan L, Yu JT (2016) TREM2
569 Overexpression has No Improvement on Neuropathology and Cognitive Impairment in Aging
570 APPswe/PS1dE9 Mice. Mol Neurobiol.
571 Jonsson T et al. (2013) Variant of TREM2 associated with the risk of Alzheimer's disease. N Engl J Med
572 368:107-116.
573 Kang W, Balordi F, Su N, Chen L, Fishell G, Hébert JM (2014) Astrocyte activation is suppressed in both
574 normal and injured brain by FGF signaling. Proceedings of the National Academy of Sciences
575 111:E2987-E2995.
576 Karch CM, Goate AM (2015) Alzheimer's disease risk genes and mechanisms of disease pathogenesis. Biol
577 Psychiatry 77:43-51.
578 Kawabori M, Kacimi R, Kauppinen T, Calosing C, Kim JY, Hsieh CL, Nakamura MC, Yenari MA (2015)
579 Triggering Receptor Expressed on Myeloid Cells 2 (TREM2) Deficiency Attenuates Phagocytic
580 Activities of Microglia and Exacerbates Ischemic Damage in Experimental Stroke. Journal of
581 Neuroscience 35:3384-3396.
582 Kleinberger G et al. (2014) TREM2 mutations implicated in neurodegeneration impair cell surface
583 transport and phagocytosis. Science Translational Medicine 6:243ra286-243ra286.
584 Koronyo Y, Salumbides BC, Sheyn J, Pelissier L, Li S, Ljubimov V, Moyseyev M, Daley D, Fuchs DT,
585 Pham M, Black KL, Rentsendorj A, Koronyo-Hamaoui M (2015) Therapeutic effects of glatiramer
586 acetate and grafted CD115(+) monocytes in a mouse model of Alzheimer's disease. Brain
587 138:2399-2422.
588 Lill CM et al. (2015) The role of TREM2 R47H as a risk factor for Alzheimer's disease, frontotemporal
589 lobar degeneration, amyotrophic lateral sclerosis, and Parkinson's disease. Alzheimers Dement
590 11:1407-1416.
591 McGeer PL, Itagaki S, Tago H, McGeer EG (1987) Reactive microglia in patients with senile dementia of

JNeurosci Accepted Manuscript

592 the Alzheimer type are positive for the histocompatibility glycoprotein HLA-DR. Neuroscience
593 Letters 79:195-200.
594 Melchior B, Garcia AE, Hsiung BK, Lo KM, Doose JM, Thrash JC, Stalder AK, Staufenbiel M, Neumann
595 H, Carson MJ (2010) Dual induction of TREM2 and tolerance-related transcript, Tmem176b, in
596 amyloid transgenic mice: implications for vaccine-based therapies for Alzheimer's disease. ASN
597 Neuro 2:e00037.
598 Montalvo V, Quigley L, Vistica BP, Boelte KC, Nugent LF, Takai T, McVicar DW, Gery I (2013)
599 Environmental factors determine DAP12 deficiency to either enhance or suppress
600 immunopathogenic processes. Immunology 140:475-482.
601 Otero K, Shinohara M, Zhao H, Cella M, Gilfillan S, Colucci A, Faccio R, Ross FP, Teitelbaum SL,
602 Takayanagi H, Colonna M (2012) TREM2 and beta-catenin regulate bone homeostasis by
603 controlling the rate of osteoclastogenesis. J Immunol 188:2612-2621.
604 Park JS, Ji IJ, An HJ, Kang MJ, Kang SW, Kim DH, Yoon SY (2015) Disease-Associated Mutations of
605 TREM2 Alter the Processing of N-Linked Oligosaccharides in the Golgi Apparatus. Traffic
606 16:510-518.
607 Piccio L, Deming Y, Del-Aguila JL, Ghezzi L, Holtzman DM, Fagan AM, Fenoglio C, Galimberti D,
608 Borroni B, Cruchaga C (2016) Cerebrospinal fluid soluble TREM2 is higher in Alzheimer disease
609 and associated with mutation status. Acta Neuropathol.
610 Poliani PL, Wang Y, Fontana E, Robinette ML, Yamanishi Y, Gilfillan S, Colonna M (2015) TREM2
611 sustains microglial expansion during aging and response to demyelination. J Clin Invest 125:2161-
612 2170.
613 Radde R, Bolmont T, Kaeser SA, Coomaraswamy J, Lindau D, Stoltze L, Calhoun ME, Jaggi F, Wolburg
614 H, Gengler S, Haass C, Ghetti B, Czech C, Holscher C, Mathews PM, Jucker M (2006) Abeta42-
615 driven cerebral amyloidosis in transgenic mice reveals early and robust pathology. EMBO Rep
616 7:940-946.
617 Replogle RA, Chan G, White CC, Raj T, Winn PA, Evans DA, Sperling RA, Chibnik LB, Bradshaw EM,

JNeurosci Accepted Manuscript

618 Schneider JA, Bennett DA, De Jager PL (2015) A TREM1 variant alters the accumulation of
619 Alzheimer-related amyloid pathology. Ann Neurol 77(3): 469-77.
620 Schmid CD, Sautkulis LN, Danielson PE, Cooper J, Hasel KW, Hilbush BS, Sutcliffe JG, Carson MJ
621 (2002) Heterogeneous expression of the triggering receptor expressed on myeloid cells-2 on adult
622 murine microglia. Journal of neurochemistry 83:1309-1320.
623 Scott E, Simon M, Anastasi J, Singh H (1994) Requirement of transcription factor PU.1 in the development
624 of multiple hematopoietic lineages. Science 265:1573-1577.
625 Sedgwick JD, Schwender S, Imrich H, Dorries R, Butcher GW, ter Meulen V (1991) Isolation and direct
626 characterization of resident microglial cells from the normal and inflamed central nervous system.
627 Proc Natl Acad Sci U S A 88:7438-7442.
628 Suárez-Calvet M et al. (2016) sTREM2 cerebrospinal fluid levels are a potential biomarker for microglia
629 activity in early-stage Alzheimer's disease and associate with neuronal injury markers. EMBO
630 Molecular Medicine.
631 Takahashi K, Rochford CD, Neumann H (2005) Clearance of apoptotic neurons without inflammation by
632 microglial triggering receptor expressed on myeloid cells-2. J Exp Med 201:647-657.
633 Tanzi RE (2015) TREM2 and Risk of Alzheimer's Disease — Friend or Foe? New England Journal of
634 Medicine 372:2564-2565.
635 Ulrich JD, Finn MB, Wang Y, Shen A, Mahan TE, Jiang H, Stewart FR, Piccio L, Colonna M, Holtzman
636 DM (2014) Altered microglial response to Aβ plaques in APPPS1-21 mice heterozygous for
637 TREM2. Molecular Neurodegeneration 9:20-20.
638 Wang Y, Cella M, Mallinson K, Ulrich JD, Young KL, Robinette ML, Gilfillan S, Krishnan GM, Sudhakar
639 S, Zinselmeyer BH, Holtzman DM, Cirrito JR, Colonna M (2015) TREM2 lipid sensing sustains
640 the microglial response in an Alzheimer's disease model. Cell 160:1061-1071.
641 Wang Y, Ulland TK, Ulrich JD, Song W, Tzaferis JA, Hole JT, Yuan P, Mahan TE, Shi Y, Gilfillan S,
642 Cella M, Grutzendler J, DeMattos RB, Cirrito JR, Holtzman DM, Colonna M (2016) TREM2-
643 mediated early microglial response limits diffusion and toxicity of amyloid plaques. The Journal of

644 Experimental Medicine 213(5): 667-675.

645 Yuan P, Condello C, Keene CD, Wang Y, Bird TD, Paul SM, Luo W, Colonna M, Baddeley D,
646 Grutzendler J (2016) TREM2 haploinsufficiency in mice and humans impairs the microglia barrier
647 function leading to decreased amyloid compaction and severe axonal dystrophy. Neuron 90: 724-
648 739.

JNeurosci Accepted Manuscript

JNeurosci Accepted Manuscript

649 **Table 1**

Mouse Model	Age	Brain region	Approximate stage of amyloid deposition	Changes in amyloid pathology	Accumulation of myeloid cells around plaques	Inflammatory gene transcript levels	Reference
5XFAD; *Trem2*$^{-/-}$	4M	Cortex	Early-Mid	↔	↓	N/A	(Wang et al., 2016)
		Hippo-campus	Mid	↔	N/A		
5XFAD; *Trem2*$^{-/-}$	8.5M	Cortex	Mid-late	↔	↓	↓	(Wang et al., 2015)
		Hippo-campus	Late	↑	↓		
APPPS1; *Trem2*$^{-/-}$	2M	Cortex	Early	↓	↓	↔	Current Study
APPPS1; *Trem2*$^{-/-}$;*Cx3cr1*$^{GFP/+}$	3M	Unknown	N/A	N/A	↓	N/A	(Wang et al., 2015)
APPPS1; *Trem2-/-*	4M-4.5M	Cortex	Mid	↔	↓	↓	(Jay et al., 2015)
		Hippo-campus	Early	↓	↓		
APPPS1; *Trem2-/-*	8M	Cortex	Late	↑	↓	↓	Current study
		Hippo-campus	Mid-Late	↔	↓ (data not shown)	↓ (data not shown)	Current study

JNeurosci Accepted Manuscript

650 **FIGURE LEGENDS**
651
652 **Figure 1. TREM2 deficiency reduces amyloid pathology early but exacerbates it late in disease**
653 **progression.** (a) 6E10 immunoreactive area was assessed in the cortex APPPS1;*Trem2*$^{+/+}$ and
654 APPPS1;*Trem2*$^{-/-}$ mice at 2 and (b) 8 months of age. (c) Thioflavin S+ plaque number / mm^2 was assessed
655 in APPPS1;*Trem2*$^{+/+}$ and APPPS1;*Trem2*$^{-/-}$ mice at 2 and (d) 8 months of age. (e) There was a significant
656 reduction in 6E10 immunoreactive area in the cortex of 2-month-old TREM2 deficient mice (WT,
657 n=3M/2F; KO, n=3M/2F) and a significant increase in 6E10 immunoreactive area in the cortex of 8-month-
658 old TREM2 deficient mice compared to controls (WT, n=4M/2F; KO, n=4M/3F). (f) There was a trend
659 toward a reduction in the density of ThioS+ plaque number in the cortex of 2-month-old APPPS1;*Trem2*$^{-/-}$
660 cortex compared to APPPS1;*Trem2*$^{+/+}$ controls (WT, n=4M/2F; KO, n=3M/3F), but no significant
661 difference in ThioS+ plaque density in the cortex of 8-month-old TREM2 deficient mice (WT, n=4M/2F;
662 KO, n=5M/3F). (g) Analysis of 6E10+ plaque size revealed no significant differences in 2-month-old
663 TREM2 deficient mice (WT, n=3M/2F; KO, n=3M/3F), but a significant increase in 8-month-old TREM2
664 deficient mice compared to controls (WT, n=4M/2F; KO, n=4M/2F). (h) Transcript levels of human APP
665 were assessed in 2- (WT, n=4M/2F; KO, n=3M/3F) and 8-month-old (WT, n=4M/2F; KO, n=3M/3F) mice.
666 (i) Western blots were used to examine protein levels of human APP using 6E10 in cortical lysates from 2-
667 (WT, n=3M/2F; KO, n=3M/2F) and 8-month-old (WT, n=3M/2F; KO, n=3M/2F) mice. (j) APP protein
668 levels were normalized to actin and the fold change expressed to the WT for each age. Not significant (ns),
669 $p<0.05$ (*), $p<0.01$ (**).

670

671 **Figure 2. TREM2 deficiency reduces myeloid cell number.** (a) Analysis of myeloid cell markers
672 by qPCR revealed no significant changes in expression of the myeloid cell markers PU.1, Tmem119 or
673 CD45 in cortical lysates from 2-month-old APPPS1;*Trem2*$^{-/-}$ mice compared to APPPS1;*Trem2*$^{+/+}$ controls
674 (WT, n=3M/3F; KO, n=3M/3F). However, there was a trend toward reduction in expression levels of PU.1
675 and Tmem119 in 8-month-old TREM2 deficient mice and a significant reduction in CD45 expression (WT,

JNeurosci Accepted Manuscript

676 n=2M/2F; KO, n=3M/4F). (b) Immunohistochemistry for CD45 at 2 (WT, n=3M/2F; KO, n=3M/4F) (c)
677 and 8 months of age (WT, n=4M/2F; KO, n=4M/2F) revealed (d) a significant decrease in the density of
678 cells expressing high levels of CD45 in the cortex of APPPS1;*Trem2*$^{-/-}$ mice compared to
679 APPPS1;*Trem2*$^{+/+}$ controls. Not significant (ns), $p<0.01$ (**), $p<0.001$ (***).

680 **Figure 3. TREM2 deficiency reduces plaque-associated myeloid cells.** (a) Immunohistochemistry
681 for Iba1 and 6E10 was performed to assess accumulation of myeloid cells around plaques in the
682 cortex of 2- and (b) 8-month-old APPPS1;*Trem2*$^{-/-}$ and APPPS1;*Trem2*$^{+/+}$ mice. (c) Quantification of
683 confocal images from 2- and (d) 8-month-old mice (e) revealed significant reductions in the number
684 of Iba1+ cells around plaques in TREM2 deficient mice at both 2 (WT, n=3M/2F; KO, n=3M/3F)
685 and 8 (WT, n=2M/1F; KO, n=2M/1F) months of age. (f) Quantification of CD45 immunoreactive
686 area around Congo Red+ plaques in 2- and (g) 8-month-old APPPS1;*Trem2*$^{+/+}$ and APPPS1;*Trem2*$^{-/-}$
687 mice (h) revealed significant reductions in the CD45^{hi} cell accumulation around plaques in TREM2
688 deficient mice at both 2 (WT, n=3M/2F; KO, n=3M/3F) and 8 (WT, n=4M/2F; KO, n=4M/2F)
689 month time points. $p<0.01$ (**), $p<0.001$ (***).

690

691 **Figure 4. TREM2 deficiency reduces myeloid cell proliferation late in disease progression.** Mice
692 were injected with 10mg/kg BrdU IP every 24 hours for 72 hours and sacrificed 24 hours after the last
693 injection. (a) BrdU immunohistochemistry was used to identify proliferating cells in 2 and (b) 8-month-old
694 APPPS1;*Trem2*$^{-/-}$ and APPPS1;*Trem2*$^{+/+}$ mice. (c) The number of BrdU+ Iba1+ double positive cells were
695 quantified in the cortex of 2- (WT, n=1M/2F; KO, n=1M/1F) and 8-month old (WT, n=3M/1F; KO,
696 n=5M/3F) APPPS1;*Trem2*$^{-/-}$ and APPPS1;*Trem2*$^{+/+}$ mice. There were no significant differences in the
697 numbers of proliferating myeloid cells in 2-month-old TREM2 deficient mice, but there were significant
698 decreases in 8-month-old APPPS1*;Trem2-/-* mice compared to APPPS1;*Trem2*$^{+/+}$ controls. (d) Brain myeloid
699 cells were isolated from 6-9-month-old APPPS1 mice and cells were analyzed by flow cytometry. Cells were

JNeurosci Accepted Manuscript

700 gated on CD11b and (e) divided into CD45^{lo} and CD45^{hi} cells. (f) When the percent of BrdU+ cells was
701 quantified within that CD45^{hi} population, there were very few proliferating cells (0.43%). (g) However, there
702 was a substantial population (7.53%) of proliferating CD45^{lo} cells. p<0.001 (***).

703

704 **Figure 5. TREM2 deficiency reduces amyloid internalization within myeloid cells**. (a) Confocal
705 slices through amyloid plaques were acquired 1µm apart for up to 30 slices in 2- and (b) 8-month-
706 old APPPS1;*Trem2*$^{-/-}$ and APPPS1;*Trem2*$^{+/+}$ mice. The total volume of co-localization between Iba1
707 and 6E10 was measured and normalized to plaque volume. This normalized volume was
708 significantly reduced in TREM2 deficient mice at 2 (WT, n=2M/1F; KO, n=2M/1F) and 8 (WT,
709 n=1M/2F; KO, n=3M) months of age. p<0.05 (*).

710

711 **Figure 6. TREM2 deficiency reduces astrocytosis and inflammation**. (a) Immunohistochemistry
712 for GFAP and 6E10 was performed to assess astrocytosis in 2- and (b) 8-month-old APPPS1;*Trem2*$^{-}$
713 $^{/-}$ and APPPS1;*Trem2*$^{+/+}$ mice. (c) Quantification of the GFAP immunoreactive area around plaques
714 revealed significant reductions in TREM2 deficient mice at 2 (WT, n=3M/2F; KO, n=3M/3F) and 8
715 (WT, n=4M/2F; KO, n=4M/3F) months of age. (d) S100β immunoreactive area around 6E10+ plaques
716 was also examined at 2 and (e) 8 months of age and (f) revealed no significant differences between
717 genotypes at either time point (2M WT, n=3M/2F; 2M KO, n=3M/3F; 8M WT, n=4M/2F; 8M KO,
718 n=3M/2F). (g) Expression of inflammation-related transcripts was quantified using qPCR. There were
719 no significant changes in expression of these genes in TREM2 deficient mice at 2 months of age (WT,
720 n=3M/3F; KO, n=3M/3F). However, there was a significant reduction in the pro-inflammatory genes
721 IL1β and TNFα and a significant increase in the anti-inflammatory marker Fizz1 in TREM2 deficient
722 mice at 8 months of age (WT, n=2M/2F; KO, n=3M/4F). p<0.05 (*), p<0.01 (**), p<0.001 (***)

JNeurosci Accepted Manuscript

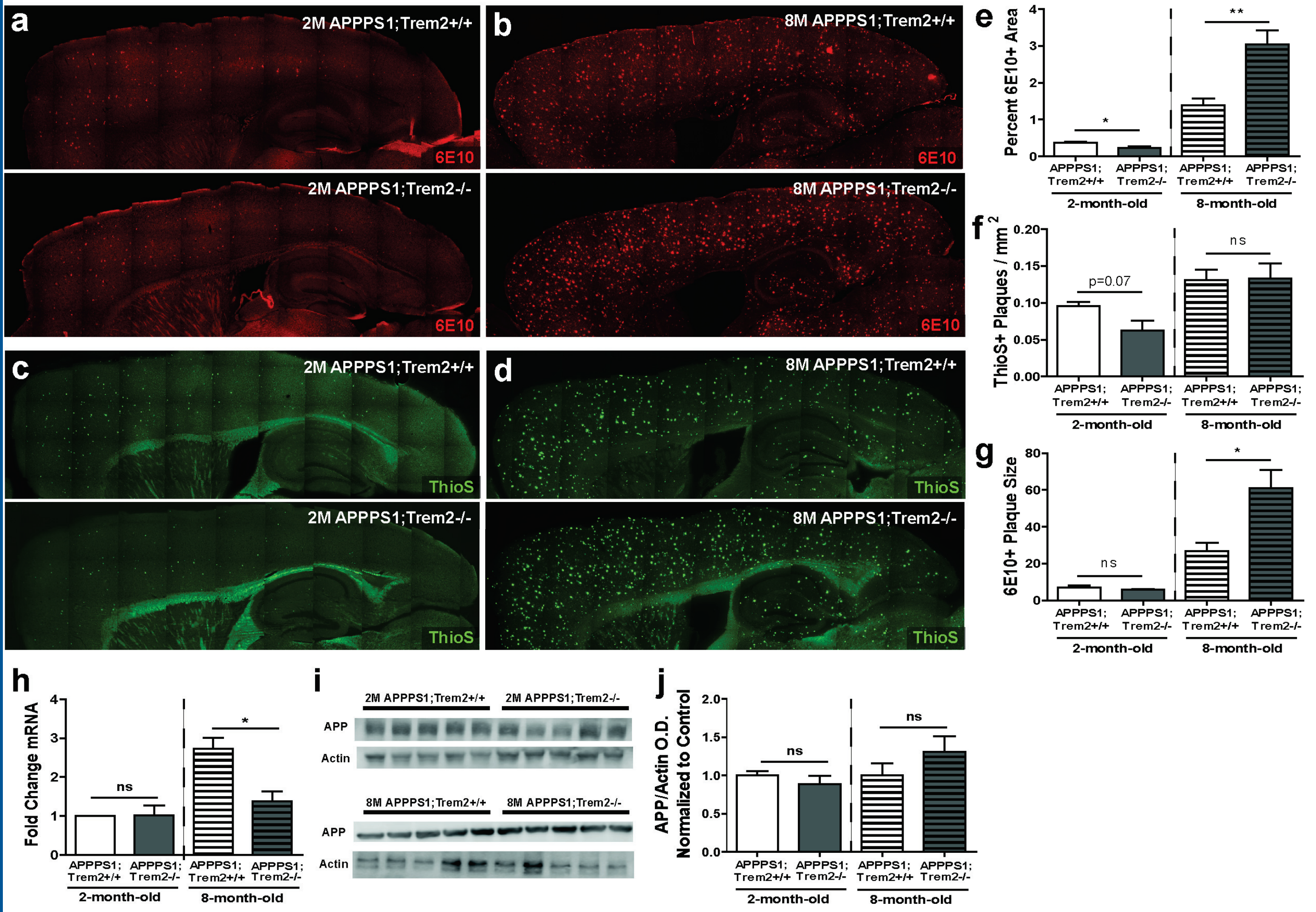

JNeurosci Accepted Manuscript

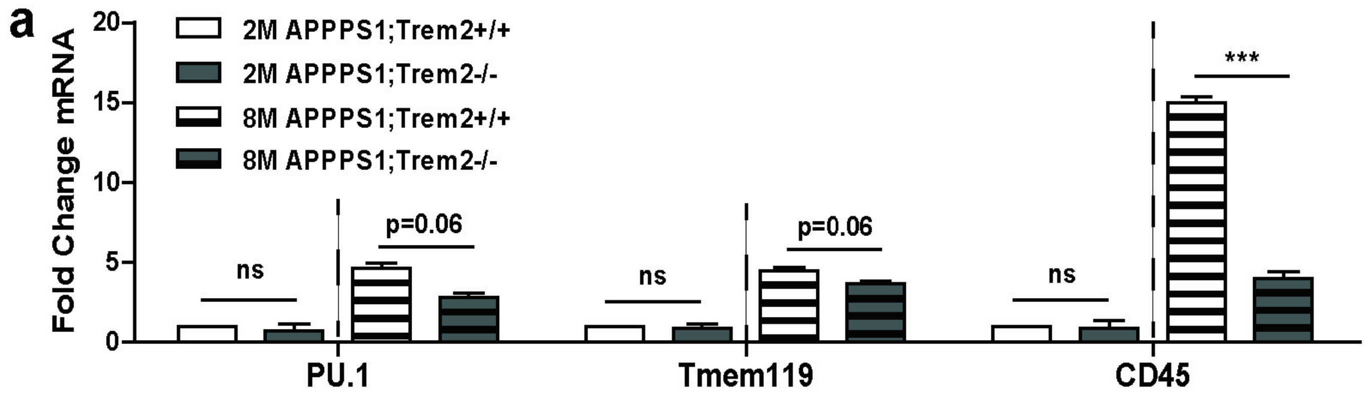

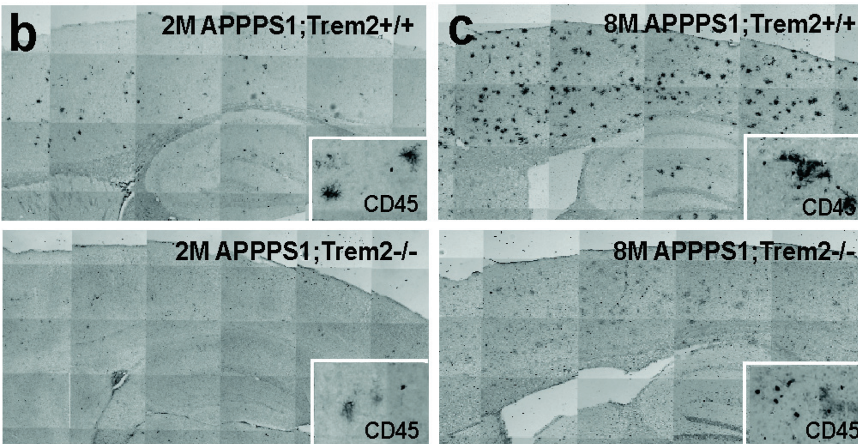

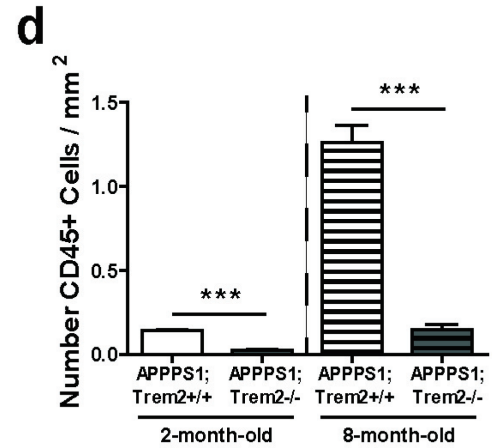

JNeurosci Accepted Manuscript

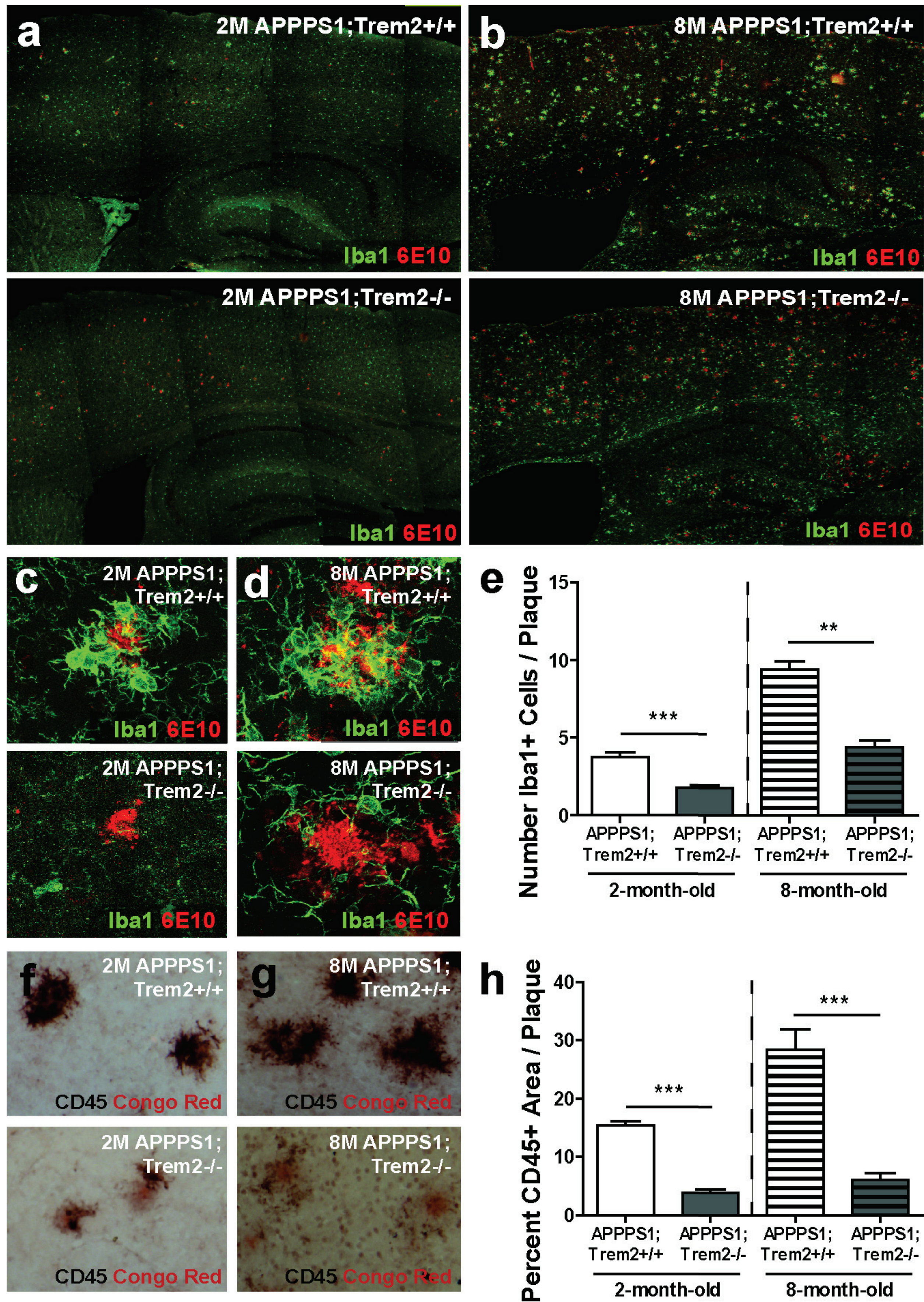

JNeurosci Accepted Manuscript

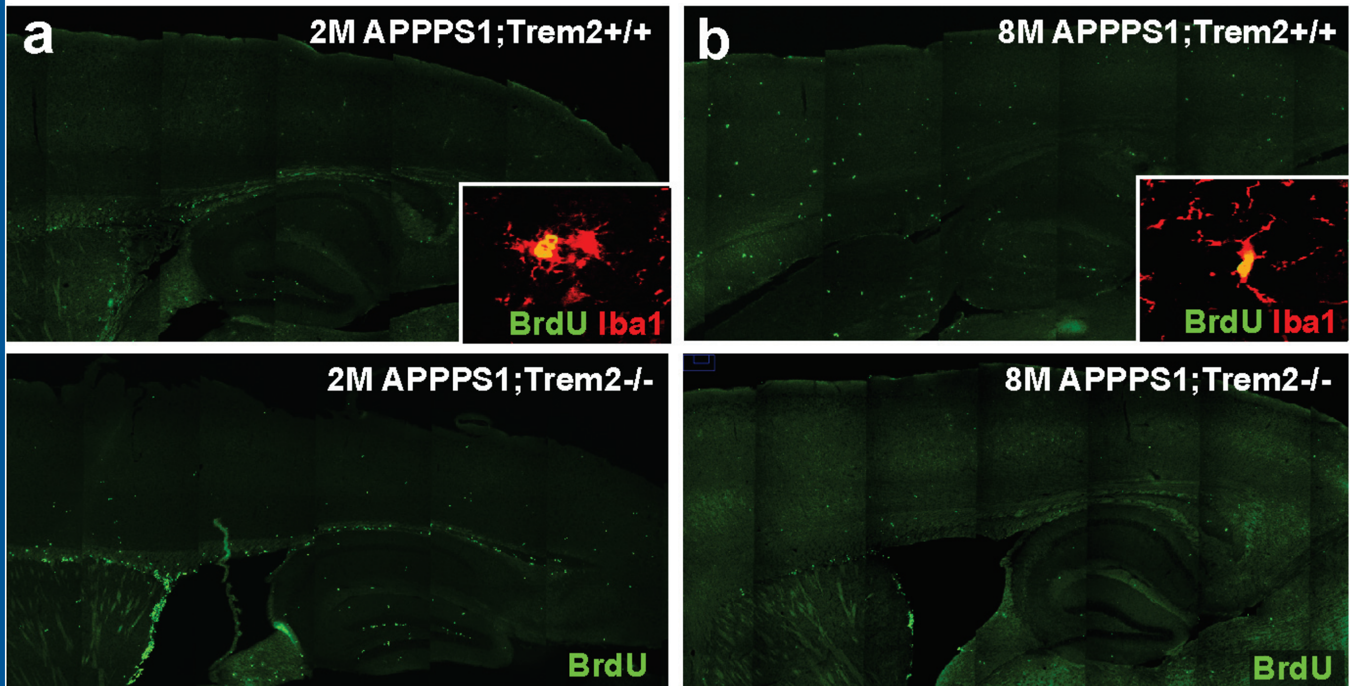

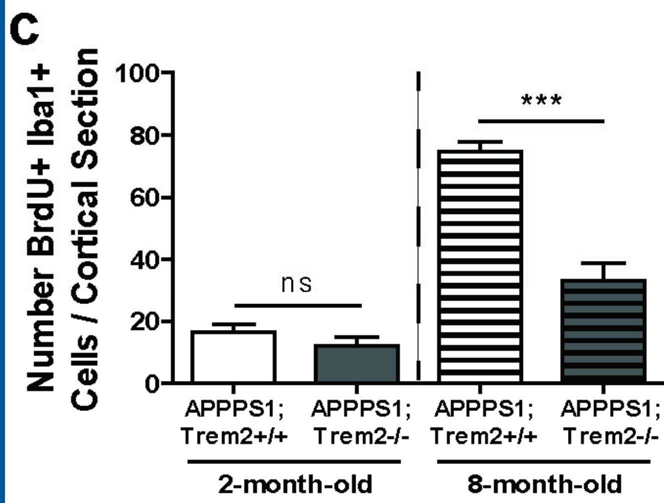

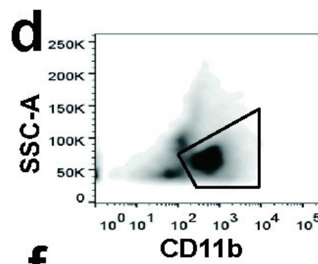

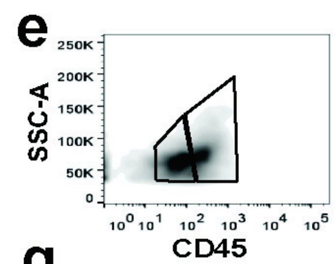

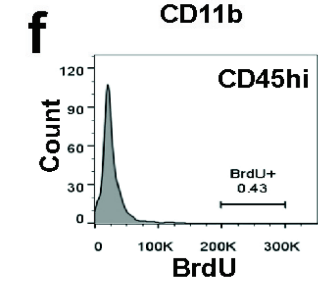

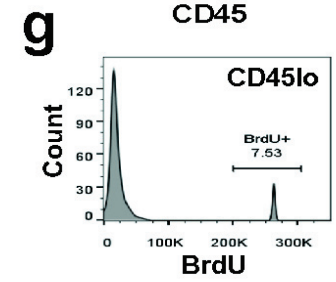

JNeurosci Accepted Manuscript

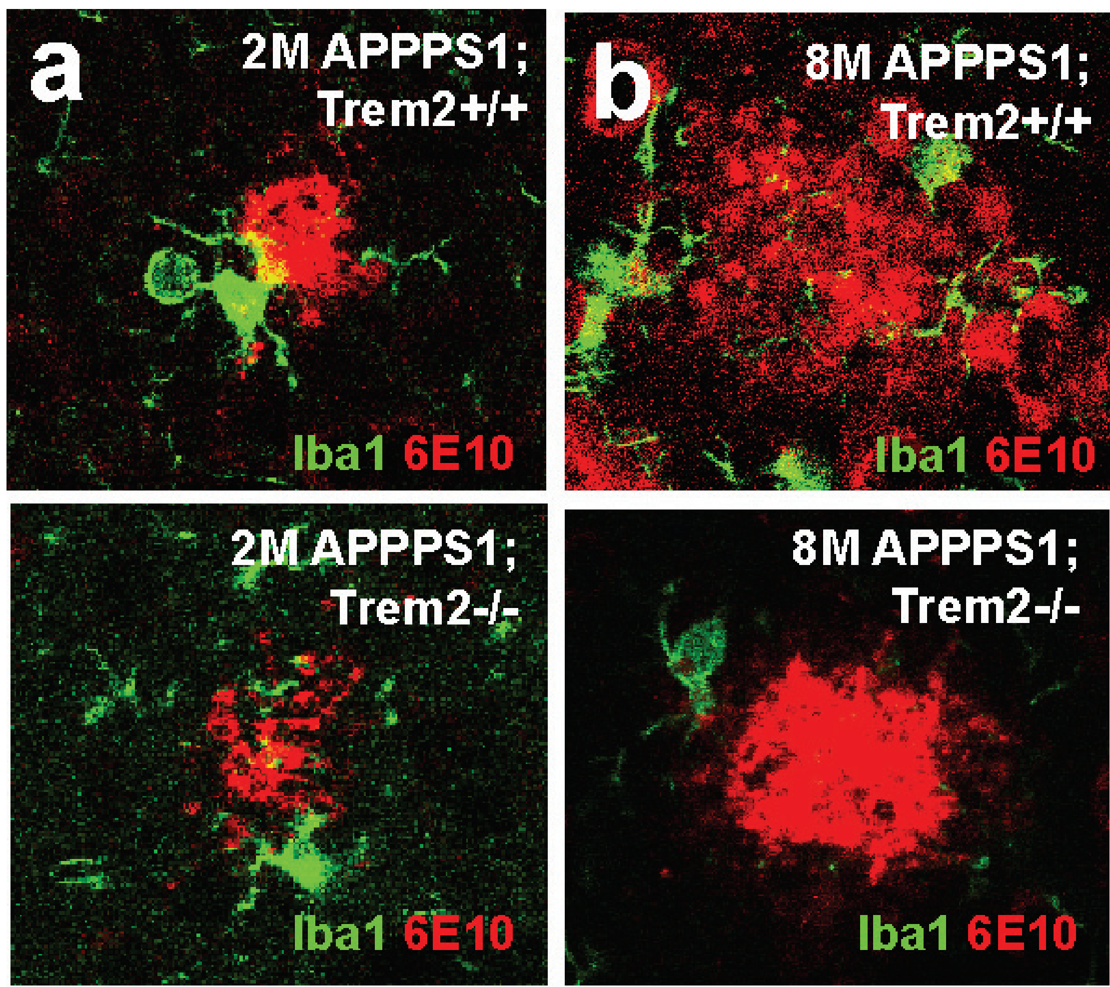

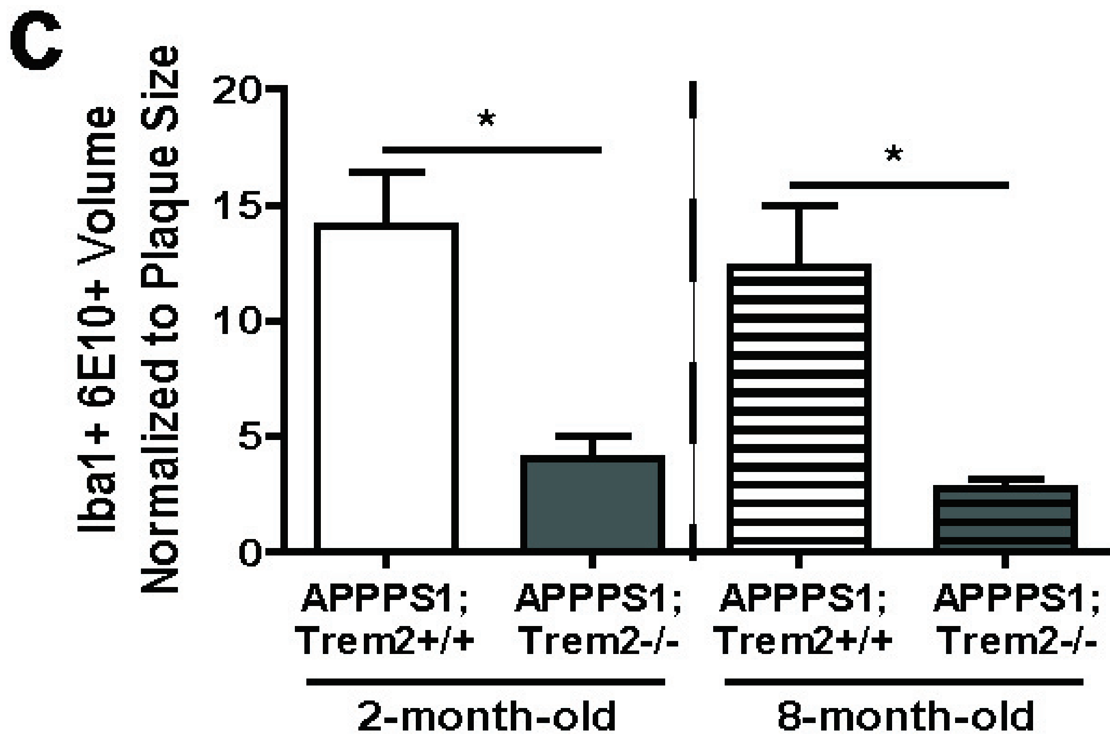

JNeurosci Accepted Manuscript